WEP Warwick Evans Publishing

International Journal of Mechanical and Electrical Engineering

ISSN: 3005-9615 (Print), ISSN: 3005-7132 (Online) | Volume 8, Number 4, Year 2026
DOI: https://doi.org/10.62051/ijmee.v8n4.05
Journal homepage: https://wepub.org/index.php/IJMEE/index

Study on Material Selection and Thermal Performance of Phase Change Materials for Lithium-Ion Batteries Adapted to Topology-Optimized Fins

Congbin Wu

key Laboratory of Railway Vehicle Thermal Engineering, School of Mechatronic Engineering, Lanzhou Jiaotong University, Lanzhou, Gansu, 730070, China

ABSTRACT

Thermal management of lithium-ion batteries is critical to ensuring their safe and efficient operation. Phase change materials (PCM) and heat transfer enhancement with fins are mainstream technical solutions at present. In this paper, a topology-optimized fin-PCM composite thermal management model is constructed for 2×3 array 18650 lithium-ion batteries. The thermal performance of three PCMs is compared via numerical simulation, and the influences of phase change temperature, latent heat and thermal conductivity on the maximum battery temperature, maximum temperature difference and liquid fraction are analyzed. The results show that PCM 2 achieves the optimal balance among latent heat capacity, phase change temperature and thermal conductivity under 3C and 4C discharge conditions. At the end of discharge, the maximum temperature of PCM 2 is reduced by 2.49% and 6.17% (3C), 8.54% and 6.12% (4C) compared with PCM 1 and PCM 3, respectively. Meanwhile, PCM 2 presents a stable liquid fraction variation and the best thermal buffering effect. This study can provide a reference for material selection and structural design of passive thermal management systems for high-rate lithium-ion batteries.

KEYWORDS

Lithium Battery; Battery Thermal Management; Phase Change Materials.

1. INTRODUCTION

Lithium-ion batteries generate heat during charging and discharging due to irreversible heat, resistance heat, and phase change heat, leading to temperature rise. In recent years, safety accidents of lithium-ion batteries have occurred frequently. For example, 18 spontaneous combustion cases of BYD vehicles were reported in the first half of 2022, ranging from smoke emission to explosion. Thermal runaway is usually triggered by high temperature, short circuit, high-rate charging and discharging, etc., which induces a chain exothermic reaction, and heat accumulation may result in deflagration.

The optimal operating temperature range of lithium-ion batteries is 15℃ to 35℃. At 45℃, the capacity decreases by 10%–20% in the short term and the service life reduces by 20%–30% compared with that at 25℃. Thermal runaway is likely to occur when the temperature exceeds 70℃. Low temperature causes capacity fading, increased internal resistance and lithium dendrite growth [1]. In addition, every 5℃ increase in temperature difference within the battery pack leads to 1.5%–2.0% capacity loss, aggravates cell inconsistency and reduces energy utilization efficiency [2]. Efficient thermal management can maintain the temperature in the optimal range, delay degradation, prolong service life, cut costs, and significantly lower the risk of thermal runaway. At present, thermal

management has become the core bottleneck restricting the development of lithium-ion batteries, and relevant research is of great significance to ensuring safety and promoting the new energy industry.

Phase change materials (PCM) are widely used in battery thermal management systems (BTMS) owing to their advantages of small temperature rise during phase change, large latent heat and good recyclability. PCM-based systems feature low cost, mature technology and excellent temperature uniformity, which can effectively suppress thermal runaway caused by local overheating. PCMs are mainly classified into organic, inorganic and eutectic types [3].Current research focuses on heat transfer enhancement of PCM. Moaveni et al. [4] encapsulated 18650 batteries in PCM and added 3% nanoparticles, reducing the maximum temperature by 0.78–1.28℃. Fins can delay PCM melting, especially at high rates, and copper foam shows remarkable cooling effect. Zhang et al. [5] optimized the fin structure and found that increasing the coverage area, the number of side fins and adding inner and outer arcs could reduce battery temperature. Chen et al. [6] designed movable fins to strengthen convection of liquid PCM, reducing the average temperature by 2% and the maximum temperature difference by 21% after discharging compared with conventional air cooling. Song et al. [7] proposed a BTMS combining air cooling and double-layer PCM, which can control the maximum temperature below 40.5℃ and keep the temperature difference within 1.09℃ with favorable temperature uniformity.

Accordingly, this paper takes 18650 cylindrical lithium-ion batteries as the research object and carries out the optimization of PCM suitable for topology-optimized fins. Numerical simulation is adopted to systematically analyze the synergistic heat transfer characteristics of topology-optimized fins and PCMs with different thermophysical properties. The influences of key PCM parameters on the maximum temperature, maximum temperature difference and liquid fraction of the composite system are clarified, and the optimal matching PCM is selected. The thermal performance improvement mechanism of the topology-optimized fin-PCM composite system is revealed. This research provides a theoretical basis and technical support for material selection and structural optimization of passive lithium-ion battery thermal management systems under high-rate discharge.

2. BTMS CONSTRUCTION AND ANALYSIS

2.1. BTMS Model Construction

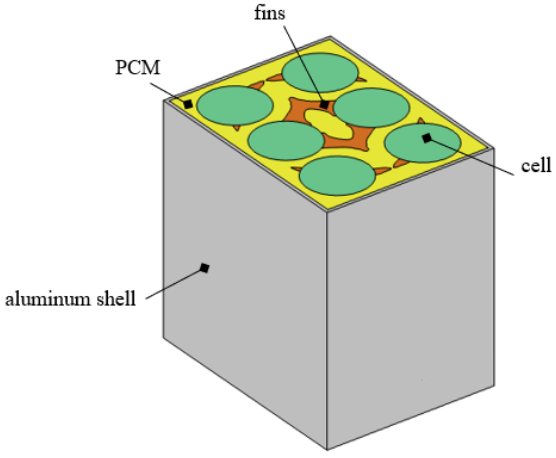

Fig 1. Structure Diagram of the BTMS Model

In this paper, a PCM-based BTMS model is established for 18650 lithium-ion batteries with a 2×3 array (6 cells in total). An aluminum shell is adopted to prevent PCM leakage, and each battery cell is treated as a cylinder. Metal fins are inserted between the battery cells and PCM to enhance heat conduction, and the heat storage capacity of PCM is utilized to absorb heat generated by the batteries

for module cooling. The metal fins adopt a topology-optimized structure with a height of 65 mm, which are distributed in the BTMS and contact both the outer surface of the batteries and the inner surface of the aluminum shell. The thermal physical parameters of the battery, metal fins and aluminum shell are listed in Table 1.

The distances between adjacent batteries are 2 mm and 7 mm, respectively. The PCM thickness at the model center is 7 mm, while that around the periphery is 2 mm, and the thickness of the battery module shell is 1 mm. The structure of the model is shown in **Fig 1**.

Table 1. Thermal Properties of Materials [8]

Material	Thermal conductivity [W/(m·K)]	Density [kg/m^3]	Heat capacity [J/(kg·K)]
Shell (Aluminum)	170	2700	875
Fin (Copper)	380	8900	385
Cell	x, y: 40.1 z: 1.1	2521.8	1191.9

2.2. BTMS Model Construction

PCM selection should consider phase change temperature, latent heat and stability. The melting point must match the optimal working conditions of batteries. An excessively low melting point leads to premature exhaustion of latent heat, whereas an overly high one fails to absorb heat in time and causes temperature rise. High latent heat can buffer the heat generated during high-rate discharge. Excellent thermal stability and cycle life prevent phase separation and thermal conductivity degradation, ensuring long-term reliability. Therefore, only by achieving the optimal balance among latent heat, thermal conductivity, phase change temperature and stability can PCM cooperate with topology-optimized fins to maximize the temperature control and uniformity performance of BTMS. In this paper, three PCMs are compared to select the most suitable one for subsequent BTMS optimization. The thermophysical parameters of the PCMs are listed in **Table 2**.

Table 2. Physical Properties of Different PCMs

Physical Parameters	PCM 1	PCM 2	PCM 3
Solid density [kg/m³]	900	900	934.6
Liquid density [kg/m³]	850	700	702
Specific heat (solid)[J/(kg·K)]	1780	1929	2156
Specific heat (liquid)[J/(kg·K)]	2146.7	2383	2156
Thermal conductivity (solid) [W/(m·K)]	0.22	0.317	0.4
Thermal conductivity (liquid) [W/(m·K)]	0.13	0.205	0.19
Phase change latent heat [J/kg]	113000	249000	237320
Melting point [°C]	35	37.8	41

3. NUMERICAL MODEL CONSTRUCTION

3.1. Model Assumptions

To establish an accurate lithium-ion battery model, proper simplifications are made before simulation. The specific assumptions are as follows:

(1) The physical properties of battery materials are uniform and constant.

(2) The battery is regarded as a uniform heat generator with uniform current distribution during operation.

Based on the above assumptions and the foregoing content, the energy conservation equation of the battery can be derived as:

$$\rho_{\text{cell}} V_{\text{cell}} c_{\text{P,cell}} \frac{\partial T}{\partial t} = Q_{\text{total}} - Q_{\text{loss}} \tag{1}$$

Where V_{cell} is the volume of the simplified battery in m^3, and Q_{loss} is the heat loss of the battery in W, whose calculation formula is

$$Q_{\text{loss}} = 2hA_{\text{cell}}(T_{\text{avg}} - T_{\text{out}}) \tag{2}$$

Where A_{cell} is the surface area of the lithium-ion battery in m^2, T_{avg} is the average temperature of the battery in K, and T_{out} is the ambient temperature in K.

To verify the reliability of the single-cell heat generation model, the simulated battery temperature variation curve is compared with the experimentally measured average surface temperature data reported in Ref. [8].

3.2. Validation of Model Accuracy

In this paper, a battery thermal management model is constructed with 8 mm thick PCM and 1 mm wide aluminum fins, enclosed by a 2 mm thick acrylic outer shell. All components have a height of 65 mm. Transient simulations are carried out at an ambient temperature of 25 ℃, with boundary conditions and thermophysical parameters set according to the literature. The maximum temperature variations under two operating conditions are presented in Fig 2 (a). The results show that the simulated temperature curves are in good agreement with the experimental data. The relative errors are illustrated in Fig 2 (b). The relative errors under 3C and 4C conditions are both less than 5%, and the maximum temperature difference is below 2 ℃. Specifically, the maximum error is 2.95% for 3C and 4.54% for 4C, which meets the error criteria for complex coupled heat transfer problems. Thus, the accuracy and reliability of the proposed model are verified

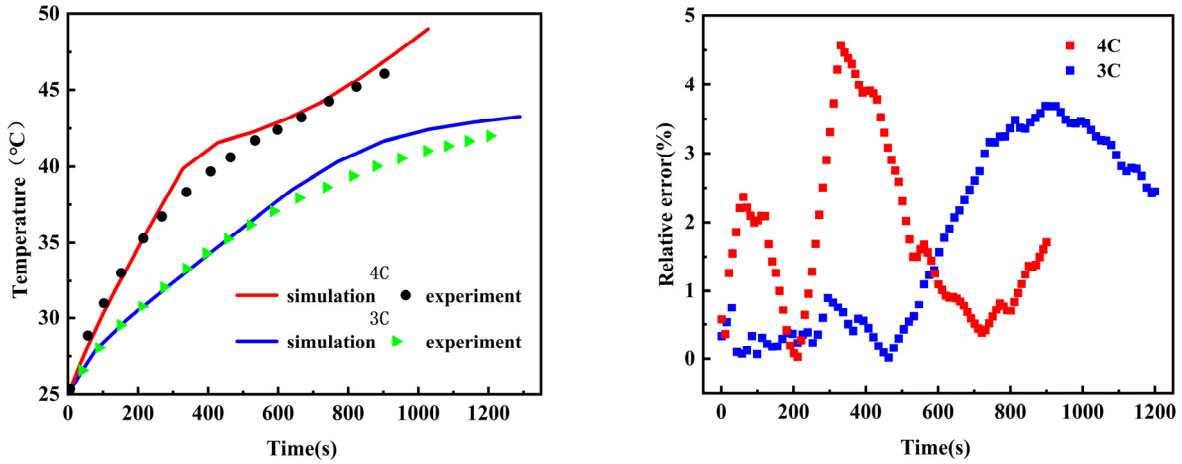

(a) Simulation and Experiment under 3 C and 4C (b) Relative Errors under 3 C and 4 C

Fig 2. Comparison and Relative Error between Simulation and Literature Results

3.3. Grid Independence and Time Step Independence Analysis

Grid quality directly determines the calculation accuracy and convergence. Refining the grid improves the precision in capturing physical quantities, but significantly increases the solution scale and computing time. In this work, a lithium-ion battery PCM thermal management model is established in COMSOL. Grid independence analysis is performed at 25 ℃ under 3C discharge condition with three grid numbers: 101621, 158217 and 199004. The variation trend is shown in Fig 3. The results indicate that the average battery temperature changes gently when the grid number exceeds 101621. Considering both accuracy and efficiency, 158217 elements are finally adopted.

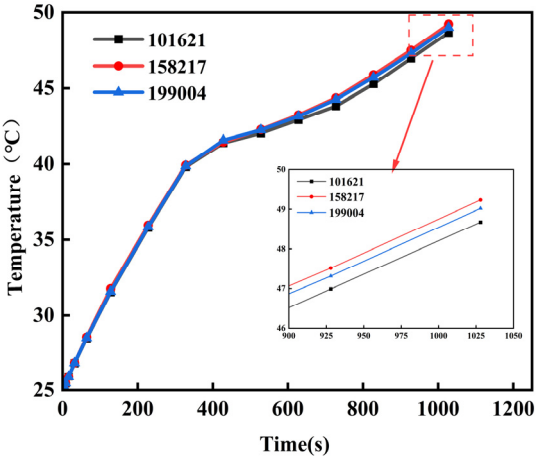

Fig 3. Grid Sensitivity Analysis of Numerical Model

Time step is also critical. As shown in Fig 4, an excessively small time step reduces efficiency and accumulates errors, while an overly large one fails to capture transient variations and may even skip key processes such as PCM melting. Under the same working conditions, three time steps (0.5 s, 1 s, and 1.5 s) are compared. The temperature rise curves of 0.5 s and 1 s are highly consistent, whereas the 1.5 s step underestimates temperature due to insufficient resolution of the transient coupling between heat generation and PCM thermal storage. After comprehensive evaluation, this study adopts a 158217 grid with a 1 s time step for subsequent simulations, which ensures the accuracy of transient thermal behavior calculation and effectively controls computational complexity, achieving an optimal balance between accuracy and efficiency

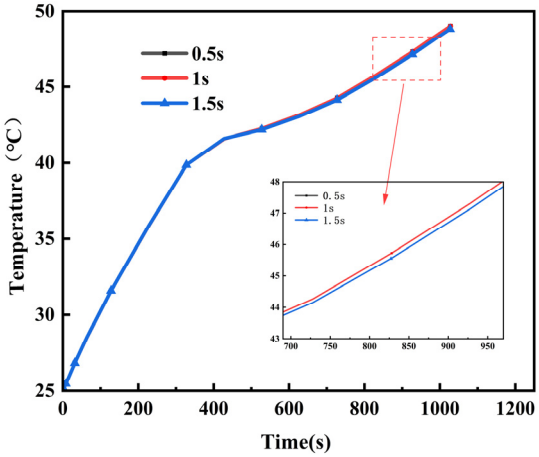

Fig 4. Time Step Independence Verification of the Numerical Model

4. RESULTS AND DISCUSSION

4.1. Comparison of Maximum Temperature for Different PCMs

Fig 5 shows the variation curves of the maximum battery module temperature with three phase change materials combined with topology-optimized fins under 3C and 4C conditions. The temperature control performance of the battery module is jointly determined by the operating conditions and the thermophysical properties of PCMs.

Under 3C condition, PCM 3 exhibits the fastest temperature rise in the early stage due to the highest phase change temperature, and its cut-off temperature remains relatively high in the later stage despite heat absorption. PCM 1 shows the lowest temperature in the early stage owing to the low phase change point, but its temperature rises sharply at the end because latent heat is exhausted and liquid-phase thermal conductivity is poor. PCM 2 can continuously and steadily absorb heat after passing the phase change point until the end of discharge due to its high latent heat capacity.

Under 4C high-rate condition, the heat generation of the battery increases significantly. PCM 2 and PCM 3 effectively buffer the temperature rise within about 850 seconds relying on large latent heat and high thermal conductivity. However, the heat generation rate surges due to increased internal resistance, leading to a steep rise in temperature curves. PCM 1 experiences an earlier rapid temperature rise because insufficient latent heat and decreased driving force of liquid-phase heat conduction result in an imbalance between heat dissipation and heat generation. Quantitative results demonstrate that at the discharge cut-off point, the maximum temperature of PCM 2 is 2.49% lower than that of PCM 1 and 6.17% lower than that of PCM 3 under 3C condition; under 4C condition, the reductions are 8.54% and 6.12%, respectively.

In summary, PCM 2 achieves the optimal balance among latent heat capacity, thermal conductivity and phase change temperature, with the highest temperature control efficiency and strong condition adaptability. Therefore, PCM 2 is the best matching phase change material for the topology-optimized fin structure in this study.

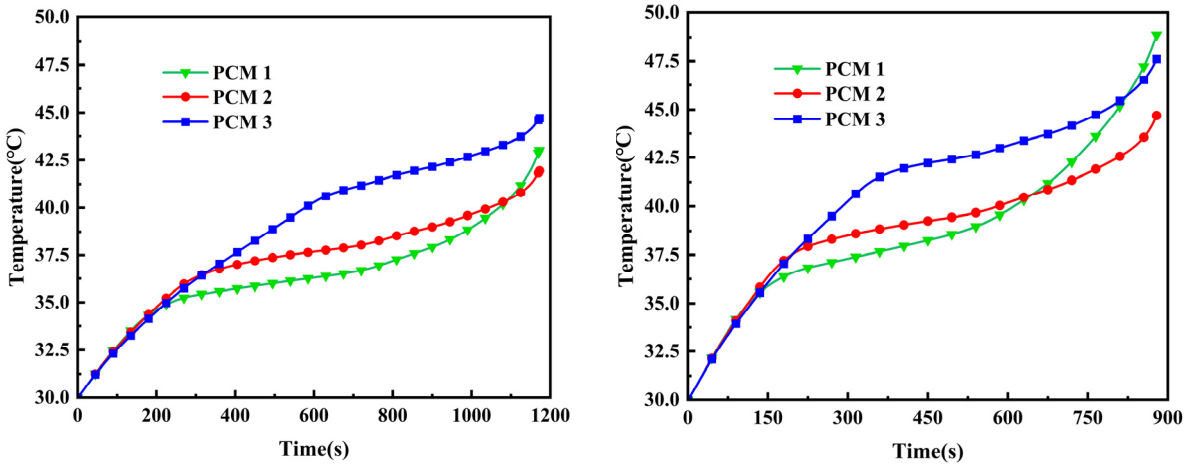

Fig 5. Maximum Comparison of Battery Temperatures with Different PCMs Under Various Operating Conditions. (a) 3 C; (b) 4 C

4.2. Comparison of Maximum Temperature Difference for Different PCMs

Fig 6 shows the variation of the maximum temperature difference in the battery module using three different phase change materials under 3C and 4C operating conditions.Under 3C condition, at the

initial stage of discharge, the maximum temperature difference of the battery module with PCM 1 is much higher than that with the other two PCMs between 180 s and 320 s, owing to the low solid-phase thermal conductivity of PCM 1. However, during the subsequent discharge process, the maximum temperature difference of the battery module using PCM 1 remains the lowest.The reason is that the phase change temperature of PCM 1 is 35 ℃, which matches well with the optimal operating temperature range of the battery. During the entire discharge process, the battery temperature fluctuates around the phase change temperature of PCM 1, allowing PCM 1 to continuously absorb heat through latent heat and thus suppress local overheating. Even after the latent heat is consumed, the relatively low phase change temperature leads to a uniform temperature field in the battery module, maintaining a low maximum temperature difference.

This phenomenon still exists under 4C condition. The maximum temperature difference of the battery module results from the synergistic effect of phase change temperature, thermal conductivity and latent heat capacity of PCMs. The battery module with PCM 1 still presents the lowest maximum temperature difference among the three PCMs.With its low phase change temperature, PCM 1 starts to regulate the battery temperature via latent heat at an earlier stage. In contrast, although PCM 2 and PCM 3 possess higher latent heat capacity and thermal conductivity, their higher phase change temperatures result in a delayed latent heat buffering effect until the late discharge stage. As the battery temperature exceeds their phase change temperatures, the latent heat buffering weakens, and the higher overall temperature tends to enlarge the temperature difference.

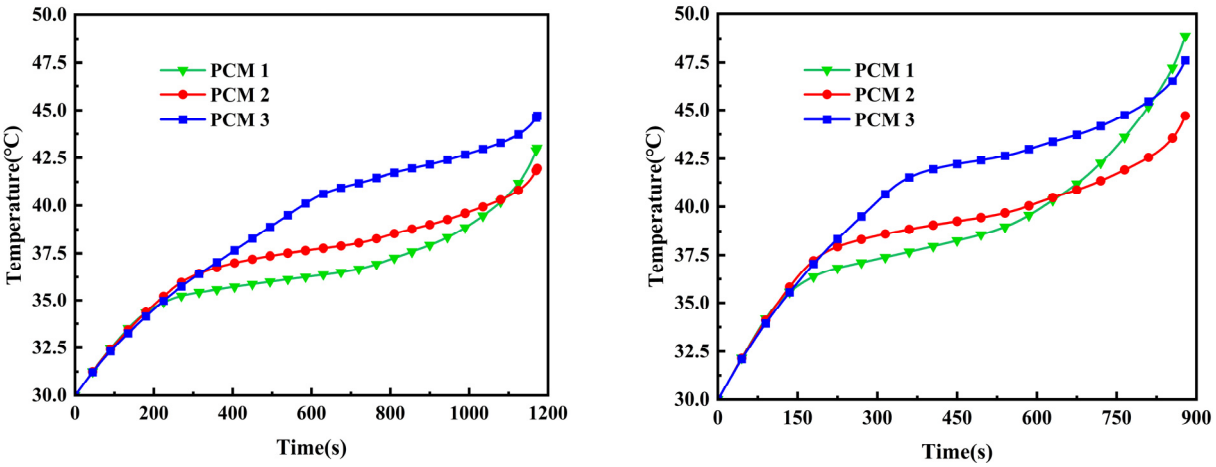

(a) (b)

Fig 6. Maximum Temperature Difference of Battery Packs with Different PCMs under Two Operating Conditions. (a) 3C; (b) 4C.

4.3. Comparison of Liquid Fraction for Different PCMs

Fig 7 shows the variation curves of liquid fraction for the three phase change materials with discharge time under 3C and 4C conditions. Liquid fraction is a key indicator characterizing the degree of latent heat release, which directly reflects the heat absorption efficiency and thermal buffering capacity of the system.Under 3C discharge condition, the liquid fraction of all three PCMs increases with discharge time, reaching approximately 0.56, 0.35 and 0.30 at the cut-off moment, respectively. Owing to its lower phase change temperature and higher thermal conductivity, PCM 1 exhibits the fastest growth in liquid fraction, leading to premature exhaustion of latent heat and insufficient thermal management in the later discharge stage. The liquid fraction of PCM 2 and PCM 3 increases gently, with PCM 2 consistently higher than PCM 3, showing better thermal buffering potential.

Under 4C high-rate condition, the heat generation rate increases sharply, and the liquid fraction of all three PCMs rises much more rapidly, finally reaching about 0.65, 0.40 and 0.38, respectively. The

trend is similar to that under 3C: PCM 1 is limited by its thermophysical properties and fails to suppress the severe temperature rise; PCM 3 shows the slowest growth and the lowest final value, indicating poor matching between latent heat capacity and phase change temperature. PCM 2 presents moderate and stable growth, and its phase transition process is well matched with the rapid heat flow, enabling continuous heat absorption under intense heat generation and giving full play to its latent heat advantage.

In summary, PCM 2 demonstrates the best latent heat utilization characteristics under both operating conditions. Its liquid fraction evolution is highly consistent with heat generation, providing stable thermal buffering for both low-medium and high-rate discharges. This conclusion agrees well with the temperature field distribution presented earlier, strongly verifying that PCM 2 is the optimal material for the BTMS in this study.

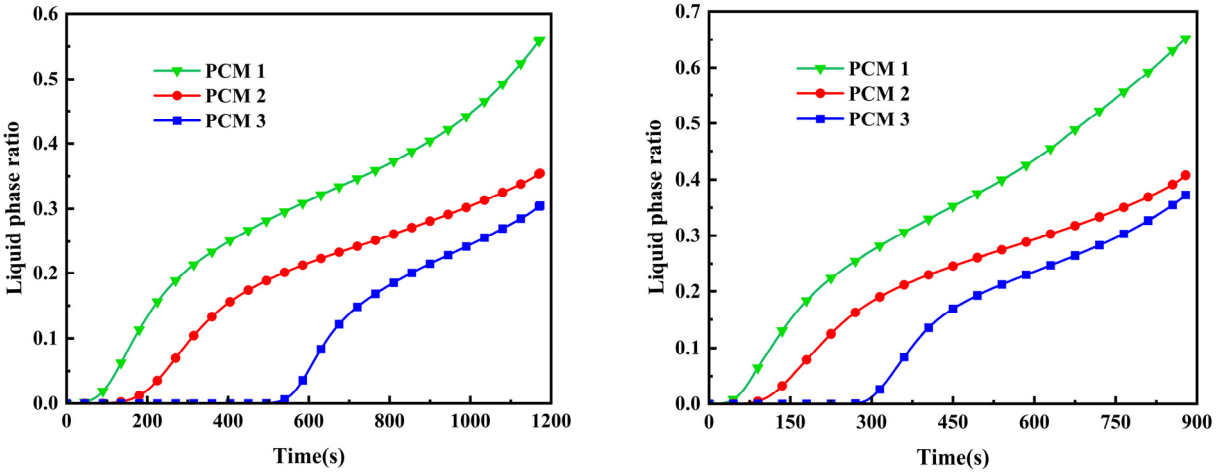

(a) (b)

Fig 7. Liquid Fraction of Battery Packs with Different PCMs under Two Operating Conditions. (a) 3C; (b) 4C.

5. SUMMARY

Taking 18650 cylindrical lithium-ion batteries as the research object, this paper establishes a thermal management model coupling topology-optimized fins with phase change materials. Numerical simulations are conducted to compare the thermal performance of three PCMs under 3C and 4C discharge conditions, revealing the influences of phase change temperature, latent heat and thermal conductivity on temperature control, temperature uniformity and latent heat utilization efficiency of the battery module.

Results show that PCM 1 has a low phase change temperature and the best temperature uniformity, but suffers from small latent heat and poor liquid-phase thermal conductivity, leading to rapid temperature rise due to premature latent heat exhaustion at high discharge rates. PCM 3 exhibits a relatively high phase change temperature, resulting in fast initial temperature increase and weak overall temperature control performance. In contrast, PCM 2 achieves the optimal balance among phase change temperature, latent heat capacity and thermal conductivity. It effectively suppresses the maximum battery temperature under both 3C and 4C conditions, with remarkable temperature control advantages at the late discharge stage. The stable liquid fraction evolution and reliable thermal buffering capacity enable PCM 2 to adapt to intense heat generation under high-rate discharge.

Through model validation and parameter optimization, the composite system combining topology-optimized fins with PCM 2 maintains the battery temperature within a safe range, improving the reliability and service life of thermal management. The findings can provide theoretical support and

technical reference for material selection and structural design of passive thermal management systems for high-rate lithium-ion batteries.

REFERENCES

[1] Hu X, Zheng Y, Howey A D, et al. Battery warm-up methodologies at subzero temperatures for automotive applications: Recent advances and perspectives[J]. Progress in Energy and Combustion Science, 2020, 77: 100806-100806.

[2] Iraola, Unai, Aizpuru, et al. Influence of Voltage Balancing on the Temperature Distribution of a Li-Ion Battery Module[J]. IEEE Transactions on Energy Conversion, 2015, 30 (2): 507-514.

[3] Luo D., Zhao Y., Cao J., et al. Performance analysis of a novel thermoelectric-based battery thermal management system[J], Renewable Energy, 2024, 224: 120193.

[4] Moaveni A., Siavashi M, Mousavi S. Passive and hybrid battery thermal management system by cooling flow control, employing nano-PCM, fins, and metal foam[J]. Energy, 2024, 288: 129809.

[5] Zhang F., Lu F., Liang B., et al. Thermal performance analysis of a new type of branch-fin enhanced battery thermal management PCM module[J]. Renewable Energy, 2023, 206: 1049-1063.

[6] Chen G., Shi Y., Ye H., et al. Experimental study on phase change material based thermal management design with adjustable fins for lithium-ion battery[J]. Applied Thermal Engineering, 2023, 221.

[7] Song K, He R, Gao C, et al. Performance of a combined battery thermal management system with dual-layer phase change materials and air cooling technologies[J]. Applied Thermal Engineering, 2024, 254: 123865-123865.

[8] Zhang F., Lu F., Liang B., et al. Thermal performance analysis of a new type of branch-fin enhanced battery thermal management PCM module[J]. Renewable Energy, 2023, 206: 1049-1063.